PRZEMYSŁAW KRZYK, NATALIA PRAGŁOWSKA-RYŁKO, MACIEJ SUŁOWICZ[*]

APPLICATION OF INTERPOLATED DISCRETE FOURIER TRANSFORM METHOD IN THE DIAGNOSTICS OF CAGE INDUCTION MOTORS

ZASTOSOWANIE METODY INTERPOLOWANEJ DYSKRETNEJ TRANSFORMATY FOURIERA DO DIAGNOSTYKI SILNIKÓW INDUKCYJNYCH KLATKOWYCH

A b s t r a c t

This paper compares the accuracy of the multi-frequency stator phase current spectrum estimation. This is as a development of considerations made in [1]. In this paper, the authors added to previous results for the classic Discrete Fourier Transform method and the two-point interpolated DFT method (IpDFT), new results obtained by three-point IpDFT method's algorithm. The analysis was made for slip spectrum component which is used for cage damage detection. To minimize the spectrum leakage effect, the selected Rife-Vincent Class I windows (RVCI) were used. The article focuses on the effectiveness of spectral component estimation in function of the used method, type of time window and measurement time. Values of errors of frequency and amplitude estimations are presented on graphs. The authors compared theoretical considerations with the case of real stator current of an asynchronous motor with a broken cage. This article can be used as a base for further studies on the diagnosis of induction motors.

Keywords: *Discrete Fourier Transform (DFT)*, *two and three-point IpDFT method*, *estimation of signal parameters*, *spectral leakage*, *time windows RVCI*, *diagnosis of electrical motors*

S t r e s z c z e n i e

Niniejszy artykuł przedstawia porównanie dokładności estymacji parametrów dla sygnału wieloharmonicznego. Artykuł jest rozszerzeniem rozważań zawartych w pracy [1]. Autorzy poszerzyli poprzednie badania wykonane dla klasycznej metody DFT i interpolowanej dwupunktowej metody DFT o kolejny algorytm – trzypunktową metodę interpolowanego DFT. Analizę przeprowadzono dla częstotliwości poślizgowej widma, którą stosuje się najczęściej do detekcji uszkodzeń silnika. W celu ograniczenia wpływu przecieku widma użyto wybranych okien Rife'a–Vincenta klasy I (RVCI). Niniejszy artykuł koncentruje się na skuteczności estymacji składowych widma w zależności od użytej metody, wykorzystanego okna czasowego i czasu pomiaru. Wartości błędów estymacji częstotliwości i amplitudy zostały przedstawione na wykresach. Autorzy porównali wyniki rozważań teoretycznych z rzeczywistym przypadkiem uszkodzenia klatki silnika indukcyjnego. Tekst ten może stanowić podstawę dalszych badań dotyczących doskonalenia metod diagnostyki silników indukcyjnych.

Słowa kluczowe: *Dyskretna Transformata Fouriera, dwu- i trzypunktowa metoda IpDFT*, *estymacja parametrów sygnału*, *przeciek widma*, *okna czasowe RVCI*, *diagnostyka silników elektrycznych*

* Ph.D. Eng. Przemysław Krzyk, M.Sc. Eng. Natalia Pragłowska-Ryłko, Institute of Electrical Engineering and Computer Science, Cracow University of Technology.
Ph.D. Eng. Maciej Sułowicz, Institute of Electromechanical Energy Conversion, Cracow Iniversity of Technology.

1. Introduction

Diagnostics of electrical motors is a widely used and developed branch of research nowadays [2–10]. The early detection of irregularities in the functioning of machines can reduce operating costs associated with unexpected failures reducing and life of equipment [2–10].

Time-frequency analysis is successfully used for the diagnostics of electrical machines. One of the basic methods is voltage and current spectral analysis by the classic DFT method [2–10]. For asynchronous motors, spectral analysis of stator phase current commonly uses a method based on the amplitude estimation of the spectrum component with the sliding-frequency $(1 - 2s)f_0$.

The accuracy of the estimated signal parameters such as amplitude and frequency, significantly determines the diagnosis quality level of electrical machines. A significant decrease of the accuracy of the DFT method occurs when a spectral leakage appears, i.e. a transfer of power from one frequency to other frequencies.

In the case of spectral leakage, extension of measurement time and adjusting by time windows are commonly used [11]. In literature, one can find methods based on increasing frequency resolution by adding zero samples at the end of the signal [12–14]. Another way of minimizing the spectral leakage, which determines the estimation error of the signal parameter, is the spectrum interpolation by two or three-point interpolated DFT methods (2p IpDFT and 3p IpDFT). These methods effects in increasing of accuracy estimation of lobe peak position [15].

In this paper, the classic DFT methods with two and three-point (2p and 3p) IpDFT are compared. The authors analysed values of the estimated parameters of the sliding harmonic calculated by all three methods, using Rife–Vincent class I windows (RVCI) of selected orders. A previous comparison of DFT with only the two-point IpDFT method is available in [1].

2. RVCI time windows

Time windows can be separated into cosine and non-cosine windows [13]. In this paper, the authors analyzed just the cosine Rife–Vincent Class I windows (RVCI) [13], which were defined by the formula:

$$w_n = \begin{cases} \sum_{m=0}^{M}(-1)^m A_m^w \cos\left(\dfrac{2\pi}{N}mn\right) & \text{if } 0 \le n < N \\ 0 & \text{if } 0 > n \vee n \ge N \end{cases} \tag{1}$$

where:
w_n – cosine Rife–Vincent Class I windows (RVCI),
N – length of the window (number of samples),
A_m^w – amplitude of the m harmonic for cosine window of M order (for $M = 0$ RVCI window is rectangular and for $M = 1$, window is Hanning).

In this paper the authors used cosine Rife–Vincent Class I windows (RVCI) [13] of the first and the third order for $M = 1$ and $M = 3$ respectively.

3. Analysis of signal parameter estimation using the IpDFT methods

The description of algorithms for the two and three-point IpDFT method in this chapter was based on [13, 16–19].

The interpolated DFT method uses two or three adjacent bins from the DFT spectrum. Bins with the maximum modules (two or three, depending on the selected IpDFT method – 2p or 3p), allow the correction δ [13]. The coefficient δ makes a correction of bin frequency ω_k to signal frequency ω_0:

$$\omega_0 = (k \pm \delta)\frac{2\pi}{N}, 0 < \delta \le 0.5 \tag{2}$$

3.1. Two-point IpDFT method

The two-point IpDFT method is based on two bins from the DFT spectrum with the maximum modules. In other words, the IpDFT method consists on determining the ratio of DFT bins modules with the greatest amplitude, analyzed by using the time window shape. As a result, one obtains the following dependence: $v_n = w_n x_n$, where v_n is windowed signal and x_n is a sinusoidal signal. The following formulas are based on the transformations made in [13].

For RVCI windows of order $M = 0, 1, 2, \ldots$, using the two-point interpolated DFT method, one calculates correction δ by the formula [16–18]:

$$\delta = \frac{(M+1)|V_{k+1}| - M|V_k|}{|V_k| + |V_{k+1}|} \tag{3}$$

where V_k is DFT spectrum.

Correction δ is used for estimation of the bin pulsation ω_0 and bin amplitude $|V(\omega_0)|$ respectively:

$$\omega_0 = \left(k \pm \frac{(M+1)|V_{k+1}| - M|V_k|}{|V_k| + |V_{k+1}|} \right)\frac{2\pi}{N} \tag{4}$$

$$|V(\omega_0)| = \frac{2\pi}{\sin(\delta\pi)} \frac{|V_k|}{S_k} \tag{5}$$

where:

$$S_{k+n} = \left| \sum_{m=-M}^{M} \frac{(-1)^{m+n} A'_m}{\delta - (m+n)} \right| \tag{6}$$

and:

$$\begin{cases} A'_m = A_0^w & \text{if } m = 0 \\[2mm] A'_m = \dfrac{A_{|m|}^w}{2} & \text{if } m \neq 0 \end{cases} \tag{7}$$

3.2. Three-point IpDFT method

The three-point IpDFT method uses three bins modules with the greatest amplitude from the DFT spectrum. According to [13], for the three-point IpDFT method and RVCI windows, one obtains the correction δ:

$$\delta = (M+1)\frac{|V_{k+1}| - |V_{k-1}|}{2|V_k| + |V_{k-1}| + |V_{k+1}|} \tag{8}$$

which is again used for estimating the bin pulsation ω_0 and bin amplitude $|V(\omega_0)|$ respectively:

$$\omega_0 = \left(k \pm (M+1)\frac{|V_{k+1}| - |V_{k-1}|}{2|V_k| + |V_{k-1}| + |V_{k+1}|} \right)\frac{2\pi}{N} \tag{9}$$

$$|V(\omega_0)| = \frac{2\pi}{\sin(\delta\pi)} \frac{|V_{k-1}| + 2|V_k| + |V_{k+1}|}{S_{k-1} + 2S_k + S_{k+1}} \tag{10}$$

where S_{k+n} is defined in formula .

4. Comparison of classic DFT method with two and three-point IpDFT method

In this section, the authors present the analysis for the simulated multi-frequency signal and the real case of the current signal from a damaged asynchronous motor.

4.1. Almost periodic signal

In order to investigate the error level using IpDFT methods, the authors allowed a spectral leakage occurrence. The spectral leakage can be obtained for a near periodic signal (a signal which does not contain an integer number of periods).

The analysis was based on the multi-frequency waveform with ten major harmonics and five sliding harmonics. The signal was defined by:

$$f = (k - ls)f_0$$
$$for \begin{cases} k = 0; & l = 1, 2, ..., 5 \\ k = 1, 2, ..., 10; & l = -5, -4, ..., 5 \end{cases} \tag{11}$$

Waveform from was characterized by $f_p/sf_0 \in \mathbf{R}\backslash\mathbf{Q}$ and $f_p/f_0 \in \mathbf{R}\backslash\mathbf{Q}$, where f_p – sampling frequency.

The signal specified in equation has irrational values of f_0 and s:

$$f_0 \cong 50.054327 \text{ Hz}$$

$$f_0 \cong 0.015643.$$

A measuring time of 100 seconds was chosen. Measuring points were selected for: 1, 2, 5, 10, 20, 50 and 100 seconds. The assumed sampling frequency is 10 kS/s. The results are presented on graphs, with a logarithmic scale.

The authors compared the error value of the bin estimation parameter, for frequency $(1 - 2s)f_0$. Error values were received from the classic DFT method and the two and three-point interpolation. This paper compares results depending on the measurement time length, obtained after using the DFT method and two and three-point IpDFT methods. For the analysis RVCI windows of order: first (Hanning, $M = 1$) and third ($M = 3$) were used.

Results for the case when the sampling frequency was not a multiple of sf_0 (f_p/sf_0 and f_p/f_0 are irrational numbers), are presented in Figs. 1–2. Figures 1–2 include analysis from DFT method and two and three-point IpDFT methods.
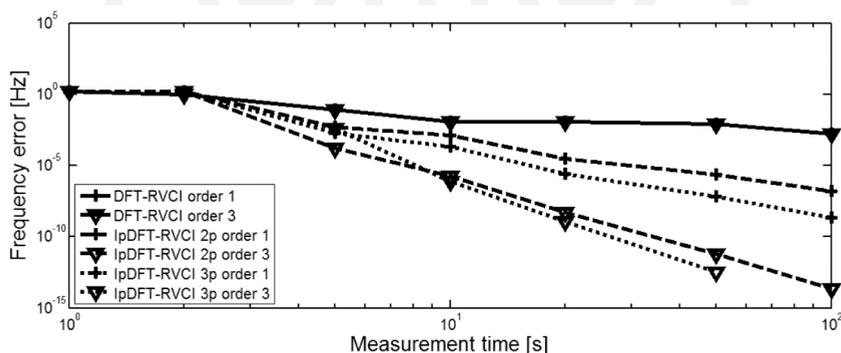
Fig. 1. Comparison of frequency error for DFT, two and three-point IpDFT method for chosen time windows
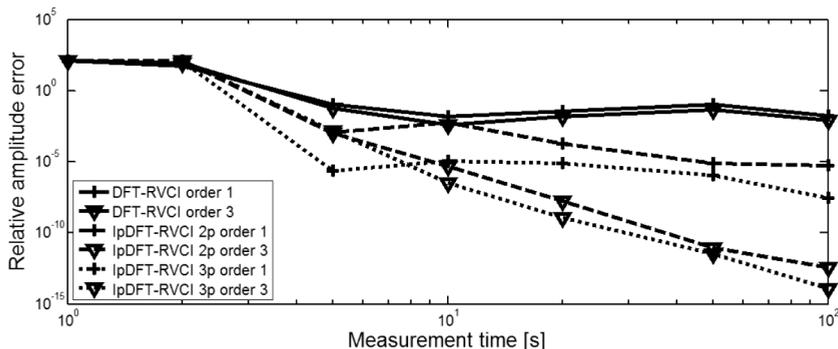
Fig. 2. Comparison of amplitude error for DFT, two and three-point IpDFT method for the chosen time windows

In the case of the frequency measurement, Fig. 1 exactly presents how the increase of the window order reduced the estimation error. It occurred for both IpDFT methods.

In the case of the classic DFT method, the window order had much less effect on the accuracy improvement.

For amplitude estimation and measurement time less than five seconds, the signal spectral analysis was practically impossible. It was caused by the spectral leakage. For measurement time longer than five seconds, the error value for IpDFT methods started to decrease. In the case of the classic DFT method, the error varied slightly during the entire measurement. Errors of measured parameters obtained from the classic DFT method can be reduced by proper selection of the windows order and the length of measurement time.

In the case of the two and three-point interpolated DFT method, the above mentioned selection can further help to reduce the measurement error [13]. Using a window of the third order, in the case of the amplitude estimation, reduces the relative measurement error value to the order of magnitude 10^{-13} for two-point IpDFT and up to 10^{-14} for three-point IpDFT.

Results obtained in Figs. 1–2 show that the two and three-point DFT interpolation method significantly improved the estimated signal parameters accuracy. This difference, however, was noticeable for measurement time longer than five seconds. For measurement time shorter than two seconds, measurement error was unacceptable for all three analyzed methods.

The authors did not use a rectangular window. For the near periodic signal, the leakage from the main bin for the rectangular window was minimal. Whereas there was a significant impact of the leakage spectrum from side lobes. Leakage from the main bin can be reduced by using a time window starting from the first order window. Figures 1–2 showed that the three-point interpolated DFT method gave better results than the classic DFT and two-point IpDFT methods for both windows of the first and third order, with measurement time extension.

4.2. Current analysis of a motor with a damaged cage

In this section, the authors present an analysis of the current signal from the transducer LEM, type HY-5, measuring one of motor phase currents with a damaged cage. The measurement was performed on the range 10 V with a resolution of 16 bits and a sampling frequency of 10 kS/s. The measurement time was 180 seconds. For frequency analysis, we used a 50 second time period, which was determined at 0.1 s. In this part, the results for the analyzed signal with the first and the third order RVCI windows are presented. For the rectangular window, the spectrum leakage was significant. This fact caused that the obtained measurement data were characterized by a high volatility and have not been presented in the article. The case of a signal spectrum with RVCI window of order 1, corresponding to the Hanning window, is presented in Fig. 3a). The signal spectrum with RVCI window of order 3 is shown in Fig. 3b).

Figure 3a) shows an extension of the main lobe and a decrease of spectrum leakage for the first order RVCI window. The reduction of spectrum leakage allowed for relatively stable measurements of signal parameters. For the third order RVCI window, Fig. 3b) shows that the main lobes were wider than in the previous cases, and some smaller value ripples disappeared. Graphs from Fig. 4 present the average value of lubricant harmonic frequency according to the first sample time. RVCI window of the first and the third order were used. All graphs are shown below, including results for the classic DFT method and the two and three-point interpolated DFT methods.

a)   b)
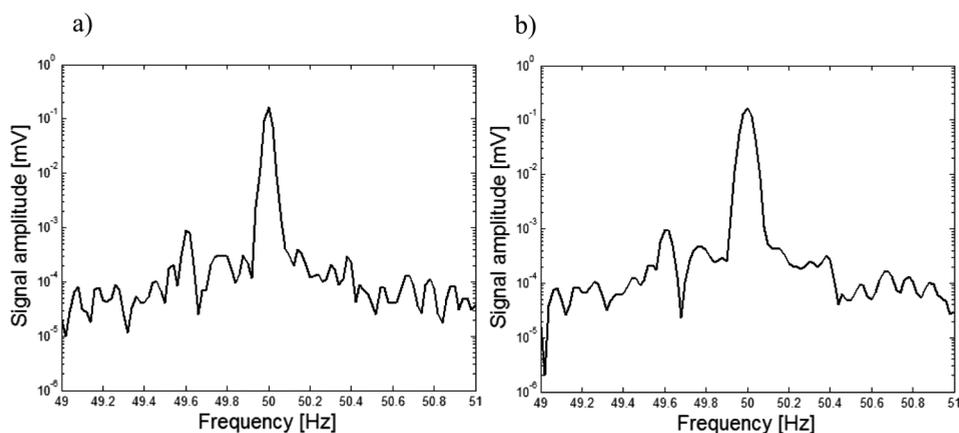
Fig. 3. Waveform of amplitude spectrum of current for the RVCI window: a) of the first order
window; b) of the third order window

a)   b)
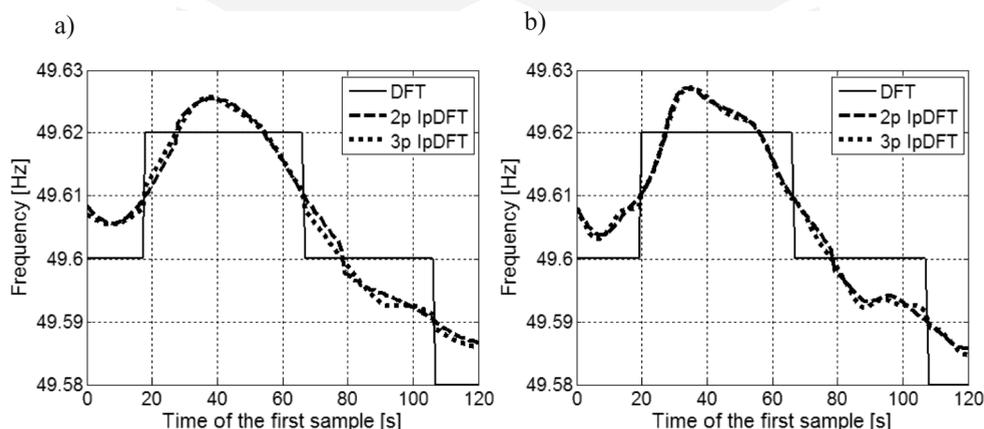
Fig. 4. Waveform of the average frequency value of the lubricant harmonic according to time of the
first sample for the RVCI window: a) of the first order; b) of the third order

The analysis shows that the frequency resolution of the classic DFT method was $1/(50\text{s}) =$ 0.02 Hz and was significantly lower than for both IpDFT methods. In addition, in the case of IpDFT methods, small fluctuations in the frequency value could be observed. For the classic DFT method, the step change of frequency was connected with the step change of the curve slope angle (second derivative discontinuity).

In Figure 5, the authors present the average value of lubricant harmonic amplitude, according to the first sample time for the RVCI window of the first and the third order.

Figure 5 shows that the value fluctuations occurred while using all presented methods, but for two and three-point IpDFT, they were significantly lower. What is more, both IpDFT methods consistently did not produce less amplitude value than the DFT method. The value difference is greater when the difference of the estimated frequency increases.

Furthermore, the curve of amplitude for the two-point IpDFT method was smoother than for the DFT method. In addition, the amplitude curve for the three-point IpDFT method

a)

b)
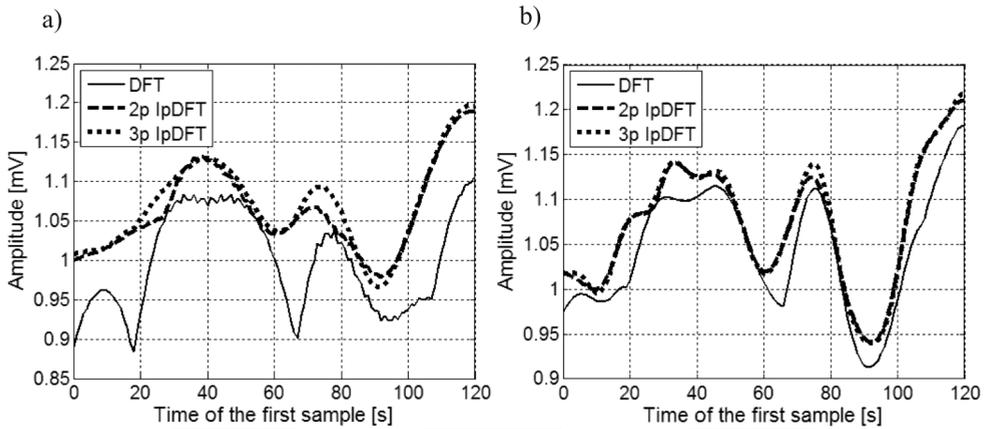
Fig. 5. Waveform of average amplitude of the lubricant harmonic depending on the first sample time for the RVCI window: a) of the first order; b) of the third order

had almost all ripples reduced. This made the three-point IpDFT more accurate in comparison with both mentioned methods. Comparing just the two and three-point IpDFT methods for the first order RVCI window, one can notice that the three-point IpDFT method gives smoother curves than the two-point IpDFT method.

Basing on Figs. 4b) and 5b), one can conclude that there is a minimization of fluctuation results for both frequency and amplitude. The obtained results were correlated with the results for the first order window. In addition, one can see the details of dynamic waveforms. As in the case of the first order window, IpDFT methods did not give less amplitude value than the classic DFT method. The difference grew with the increase of the estimated frequency. In addition, at the points of the step frequency changes, the increase of the window order had not completely wiped out a step change of the curve angle slope of the DFT waveform.

From the results one concludes that both IpDFT methods allowed estimating the lubricant harmonic value $(1 - 2s)f_0$ with a significantly higher resolution and less error than with the classic method of DFT. In addition, the window order increase allowed decreasing the spectral leakage, thereby reducing fluctuations in the received data and thus the measurement error.

Both two and three-point IpDFT methods gave quite similar results in the case of the third order RVCI window.

5. Conclusions

A comparative analysis of the advantages of different DFT methods in the diagnosis of the asynchronous motor has been achieved. It is shown how using the two and three-point IpDFT method improved the estimation accuracy of the parameters for $(1 - 2s)f_0$ bin. It is recommended to apply IpDFT methods in the case of testing low loaded engines, where the slip is uncontrolled, which implicates almost-periodic stator current.

Both two and three-point IpDFT methods can be effectively used in the diagnosis of electric machines. Particularly, the three-point IpDFT method can be the most useful because of

better fluctuation elimination. For respectively long measurement time, in the case of the real current signal from motor with damaged cage, the three-point IpDFT method gives the most reliable results from all compared methods in this article.

Moreover according to the results of the multi-frequency signal analysis, low order windows should be used for short measurement time. Analogously high order windows should be used for longer measurement time (high amount of samples). Using additionally adjusted time windows and extension of measurement time, error associated with the occurrence of the leakage spectrum can be reduced. The performed physical experiment confirmed the results obtained through simulation.

R e f e r e n c e s

[1] Krzyk P., Sułowicz M., Pragłowska-Ryłko N., *Zastosowanie IpDFT do diagnostyki silników asynchronicznych*, Zeszyty Problemowe – Maszyny Elektryczne, 2014, nr 103, BOBRME Komel, pp. 293–300.

[2] Kowalski C.T., Kanior W., *Ocena skuteczności analiz FFT, STFT i falkowej w wykrywaniu uszkodzeń wirnika silnika indukcyjnego*, Prace Naukowe Instytutu Maszyn, Napędów i Pomiarów Elektrycznych Politechniki Wrocławskiej, nr 60, Wrocław 2007.

[3] Rusek J., *Komputerowa analiza maszyny indukcyjnej z wykorzystaniem bilansu harmonicznych*, Uczelniane Wydawnictwa Naukowo-Dydaktyczne AGH, Kraków 2000.

[4] Zając M., *Metody falkowe w monitoringu i diagnostyce układów elektromechanicznych*, seria: Inżynieria Elektryczna i Komputerowa, Monografia nr 371, Politechnika Krakowska, Kraków 2009.

[5] Thomson W.T., Fenger M., *Current signature analysis to detect induction motor faults*, IEEE Ind. Appl. Mag., 2001, Vol. 7, No. 4, pp. 26–34.

[6] Głowacz A., Głowacz Z., *Diagnostics of induction motor based on analysis of acoustic signals with application of FFT and classifier based on words*, Archives of Metallurgy and Materials, 2010, Vol. 55, Issue 3, pp. 707–712.

[7] Weinreb K., Sułowicz M., Petryna J., *Kompleksowa analiza uszkodzeń wirnika w maszynach indukcyjnych metodą rozdziału widma prądu stojana*, Zeszyty Problemowe, 2000, nr 61, BOBRME, Katowice, pp. 233–238.

[8] Weinreb K., Sułowicz M., Węgiel T., *Nieinwazyjna diagnostyka wirnika maszyny asynchronicznej*, Zeszyty Problemowe, 2004, nr 69, BOBRME, Katowice, pp. 35–40.

[9] Weinreb K., *Обнаружение динамического эксцентриситета и обрыва стержней клетки в асинхронном двигателе методом спектрального анализа тока статора. Научно-технические ведомости СПбГПУ*, Основной выпуск, 2008, №1(53), pp. 119–126.

[10] Sobczyk T.J., Weinreb K., Węgiel T., Sułowicz M., Warzecha A., Maciołek W., *Ocena skuteczności diagnostyki wirników silników klatkowych na podstawie widma prądów*, Materiały 13. Konferencji Energetyki „Energetyka – modernizacja i rozwój", Kliczków, 10–12.09.2003, pp. 167–176.

[11] Harris F.J., *On the use of windows for harmonic analysis with the discrete Fourier transform*, Proc. IEEE, Jan. 1978, Vol. 66, pp. 51–83.

324

[12] Zieliński T.P., *Cyfrowe przetwarzanie sygnałów, od teorii do zastosowań*, WKŁ, Warszawa 2005.

[13] Duda K., *Fourierowskie metody estymacji widm prążkowych*, Wydawnictwa AGH, Kraków 2011.

[14] Oppenheim A.V., Schafer R.W., Buck J.R., *Discrete-Time Signal Processing*, 2nd Edition, Prentice-Hall, 1999.

[15] Schoukens J., Pintelon R., Van hamme H., *The Interpolated Fast Fourier Transform: A Comparative Study*, IEEE Trans. Instrum. Meas., April 1992, Vol. 41, No. 2, pp. 226–232.

[16] Jain V.K., Collins W.L., Davis D.C., *High-Accuracy Analog Measurements via Interpolated FFT*, IEEE Trans. Instrum. Meas., June 1979, Vol. 28, No. 2, pp. 113–122.

[17] Grandke T., *Interpolation Algorithms for Discrete Fourier Transforms of Weighted Signals*, IEEE Trans. Instrum. Meas., June 1983, Vol. 32, No. 2, pp. 350–355.

[18] Andria G., Savino M., Trotta A., *Windows and interpolation algorithms to improve electrical measurement accuracy*, IEEE Trans. Instrum. Meas., 1989, Vol. 38, pp. 856–863.

[19] Offelli C., Petri D., *Interpolation Techniques for Real-Time Multifrequency Waveform Analysis*, IEEE Trans. Instrum. Meas., February 1990, Vol. 39, No. 1, pp. 106–111.